Remote control of mechano-sensory function of primary cilia by Fe_2O_3 nanoparticles in ciliopathic animal models

R. Pala and S.M. Nauli*

Department of Biomedical & Pharmaceutical Sciences, Chapman University School of Pharmacy (CUSP), Harry and Diane Rinker Health Science Campus, Chapman University, Irvine, California 92618, United States.
Department of Medicine, University of California Irvine, Irvine, California 92868, United States.
*Email: nauli@chapman.edu; snauli@uci.edu.

ABSTRACT

In the present studies, we designed a cilia-targeted delivery system to deliver fenoldopam (FD) specifically to the primary cilia. Hence, we devised the iron oxide nanoparticle (Fe_2O_3-NP)-based technology for ciliotherapy. Dynamic light scattering measurements showed that upon surface functionalization, the size distributions were increased from 102±3.8 to 126±4.6 nm. When the surface charge of the particles was analyzed, the charge repulsion increased after every functionalization step from +12.9±2.8 to -27.9±3.4. The successful formation of bare NPs and their surface functionalization were also examined by collecting X-ray diffraction and X-ray photoelectron spectra. Live imaging confirmed that the Fe_2O_3-NPs specifically targeted primary cilia in cultured cells *in vitro* and vascular endothelia *in vivo*. Importantly, the Fe_2O_3-NPs enabled the remote control of the movement and function of a cilium with an external magnetic field, making the non-motile cilium exhibit passive movement. When used in animal models, Fe_2O_3-NPs showed significant advantage with reduced side effect compared to FD alone.

Keywords: mechano-sensory, nanoparticles, magnetism, live cell imaging, *Pkd2* mice.

1 INTRODUCTION

Primary cilia sense small changes in the surrounding microenvironment. Cilia are cellular organelles with chemo- and mechano-sensory roles [1]. Cells with dysfunctional cilia exhibit an abnormal ability to sense physical or chemical cues and may result in ciliopathies. Biochemical and molecular defects in primary cilia are associated with a wide range of diseases, including polycystic kidney disease, cancer, liver disorders, cardiovascular diseases, mental retardation, obesity, polydactyly, and retinopathy [2-5]. Because cilia are tiny cell organelles with a diameter of ~250 nm, we used haematite metal oxide (α-Fe_2O_3) as our nanomaterial due to its excellent biocompatibility, magnetic properties and applicability for use *in vivo* to target primary cilia.

In the present studies, we designed a cilia-targeted delivery system to deliver fenoldopam specifically to the primary cilia. Nanomaterials have been used for a targeted drug delivery and a sustained drug release. Nanomaterials can therefore decrease the overall drug toxicity by delivering a smaller drug dosage.

2 MATERIALS & METHODS

Most of the materials and chemicals used in our study were purchased as 97-99.9% purity and all chemicals were commercially available for purchase from Sigma-Aldrich.

All mouse experiments were performed by two operators who were blinded to the experimental conditions. All animal procedures were performed according to the University of California Irvine and Chapman University Animal Care and Use Committee Guidelines.

2.1 Cilia targeted Fe_2O_3-NPs synthesis and their characterization

The magnetic cilia targeted Fe_2O_3-NPs were prepared as previously reported [6]. Sunbright40 (OA-PEG-NHS)-functionalized nanoparticles were prepared by adding an aqueous solution of Sunbright40 (100 mg in 5 mL of d. H_2O) to the mixture and stirring it for another 24 hours at room temperature. All bare α-Fe_2O_3-NPs and Sunbright40-OA-Fe_2O_3-NPs were separated by placing a magnet (100 T) below the beaker, and the solution was allowed to clear. The particles were washed with 50 mL of nitrogen-purged sterile water three times using magnetic separation and centrifuged at low speed (1000 rpm) to remove large agglomerated particles. The dopamine receptor type-5 (DR5) antibody was generated from a synthetic peptide, and it did not cross-react with other dopamine receptors. Initially, we conjugated DR5 to AF594 maleimide using an AF594 antibody labelling kit to target thiol groups, according to manufacturer's instructions. The pre-conjugated DR5-AF594 antibody and fenoldopam were bound to the synthesized Sunbright40-OA-Fe_2O_3-NPs using a previously reported method [6].

Samples for transmission electron microscopy (TEM) analysis were prepared by placing a drop of the Fe_2O_3-NPs solution on carbon-coated copper grids. Formulated Fe_2O_3-NPs were freeze-dried and the dried powder was used for powder X-ray diffraction (XRD) and X-ray photoelectron spectroscopy (XPS) analysis. The particle size distribution and zeta potential value of the synthesized nanomaterials was analyzed using a Malvern Instruments Zetasizer Nano Series-ZS-90. The Fourier transformed infrared (FTIR) spectra were recorded using Bruker spectrometer in the diffuse reflectance mode at a resolution of 4 cm^{-1}.

2.2 Cell culture

Epithelial cells were used in this study and cultured in DMEM (Corning Cellgro, NY) supplemented with 10% FBS (HyClone, MA), and 1% penicillin-streptomycin (Corning Cellgro, NY) at 37 °C in a humidified, 5% CO_2 atmosphere. Prior to the experiments, antibiotics were withdrawn, and cells were serum starved for 24 hours to induce differentiation.

2.3 NPs targeting to cilia

The cilia targeted Fe_2O_3-NPs were evaluated by capturing images of the lateral view of both the cell body and cilium to determine the specificity of cilia targeting by NPs. Cells were grown on Formvar as previously described. Briefly, cells were grown on collagen-coated Formvar polymer film (FPF). The FPF was placed on a custom-made glass-bottomed plate. A thin pipet tip was connected to the inlet and outlet clear plastic PVC tubes. The tubes were inserted into the in-flow and out-flow pumps, and the tips were inserted between the bottom glass plate and held with a cover glass slide on its top. Different concentrations of the cilia targeted Fe_2O_3-NPs were perfused through the membrane. Different NPs targeting capabilities to the single cilia were observed with a Nikon microscope. After the NPs targeting to the cilia, it was remotely moved by external magnetic field.

2.4 Cilia length measurement

For the *in vitro* cilia length measurements, cells were grown on the formvar polymer. Primary cilia consisting of acetylated microtubule structures were measured by direct immunofluorescence staining with an acetylated-α-tubulin antibody following a 16 hours incubation with different concentrations (0.1-5 μg/mL) of cilia targeted Fe_2O_3-NPs. Likewise, the cilia targeted Fe_2O_3-NPs without loaded FD were used as the corresponding control. FD alone was also used as another control. Cells were rinsed with buffer (sodium cacodylate), fixed with 2.5% glutaraldehyde in 0.2 M buffer for 10 min, and permeabilized with 1% Triton X-100 in buffer for 5 minutes. An antibody against acetylated-α-tubulin and the secondary antibodies were also diluted in 10% FBS to decrease the background florescence; a FITC-conjugated secondary antibody.

2.5 Mouse models

One-week-old *Tie2Cre•Pkd2*$^{WT/WT}$ (with Cre activation; control group), *Tie2Cre•Pkd2*$^{flox/flox}$ (without Cre activation; control group) or *Tie2Cre•Pkd2*$^{flox/flox}$ (with Cre activation; experimental group) mice were intraperitoneally injected with 250 μg of tamoxifen in a 50-μL volume daily for five consecutive days.

Mice were treated with cilia targeted Fe_2O_3-NPs every 72 hours for 8 weeks. On the other hand, FD alone was perfused for 30 minutes every 72 hours for 8 weeks. In separate experiments, magnetic stimulation was applied every 72 hours to mice treated with cilia targeted Fe_2O_3-NPs. Five minutes after the cilia targeted Fe_2O_3-NPs injection, a 1.35-T AlNiCo cylindrical magnet was placed at the posterior and anterior regions of the mouse for 10 minutes regularly.

2.6 Blood pressure measurement

Tie2Cre•Pkd2$^{WT/WT}$, *Tie2Cre•Pkd2*$^{flox/flox}$ and *Tie2Cre•IFT88*$^{flox/flox}$ mice were subjected to blood pressure measurement by the non-invasive tail-cuff method using a CODA high-throughput system (Kent Scientific, CT). Blood pressure was measured twice daily for the duration of the study after the initial three days of acclimating to each mouse to the tail cuff. All measurements were performed by operators in a double-blind manner.

2.7 Statistical analysis

The collected data were analysed using GraphPad Prism software, version 7.0. Multiple comparisons were performed by an ANOVA followed by the Tukey post hoc test. The Bonferroni post hoc test was used to compare data between specific groups. The difference between groups was considered significant at $p < 0.05$.

3 RESULTS & DISCUSSION

We prepared stable Fe_2O_3-NPs using several synthesis steps. We analysed and characterized the materials from each synthesis and surface functionalization i.e. bare NPs to functional cilia-targeted NPs. According to the results of the dynamic light scattering (DLS) analysis, the size distributions were slightly increased following surface functionalization (**Figure 1A**). When the surface charge of the NPs was analysed, the charge repulsion increased after every functionalization step (**Figure 1B**). The zeta potential of the cilia targeted Fe_2O_3-NPs decreased to -25 mV, indicating the excellent surface stability of the cilia targeted Fe_2O_3-NPs in suspension and their suitability for intravenous applications.

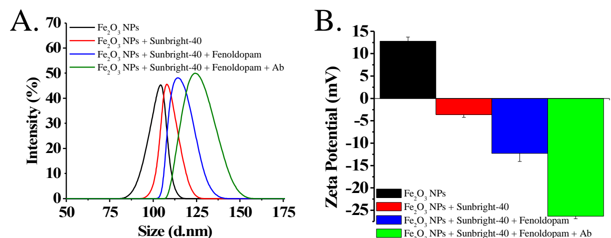

Figure 1. A) Dynamic Light Scattering analysis of Fe_2O_3-NPs and their formulations, showing the increase in size with each surface functionalization step. B) Zeta potential analysis of Fe_2O_3-NPs and their formulations, showing the increasing in negative charge with each functionalization (adapted from [6]).

The synthesized native and surface-functionalized NPs were finally compared and characterized by transmission electron microscopy (TEM) to reveal the scale and shape of the NPs before and after surface functionalization (**Figure. 2**).

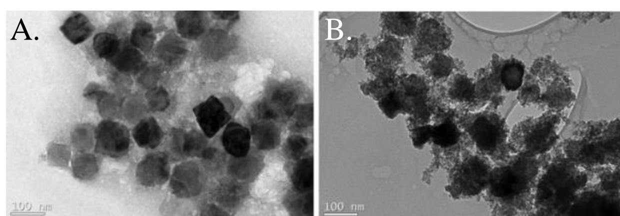

Figure 2. A. Transmission Electron Microscopy (TEM) image of bare Fe_2O_3-NPs. B. TEM image of surface functionalized Fe_2O_3-NPs.

The selectivity and specificity of the cilia targeted Fe_2O_3-NPs for primary cilia were evaluated in live cells under flow conditions (**Figure. 3A**). Prior to introducing the cilia targeted Fe_2O_3-NPs to live cells, high-resolution differential interference contrast (DIC) images were used to randomly locate a cilium. The fluorescence of the cilia targeted Fe_2O_3-NPs was measured in the cilium and cell membrane for 2 hours. After approximately one hour, the cilia surface was saturated with the fluorescent cilia targeted Fe_2O_3-NPs, while the cell membrane showed very minimal fluorescence. Based on the intensity measurements, the ratio of cilia-to-cell membrane specificity of the cilia targeted Fe_2O_3-NPs was 158±19. Importantly, primary cilia were saturated with the bound cilia targeted Fe_2O_3-NPs within one hour.

In live cells, the specificity of the cilia targeted Fe_2O_3-NPs for cilia allowed application of an external magnetic field to control non-motile cilia movement (**Figure. 3B**). The significance of this approach is that non-motile primary cilia with a "9+0" structure are able to be converted to motile-like cilia using nanotechnology to mimic nodal cells, the only known cells displaying a "9+0" ciliary structure and motility.

NPs were incubated with cells for 16 hours to further confirm the cellular effects of the cilia targeted Fe_2O_3-NPs. In addition to a phosphate-buffered saline (PBS)-treated control group (vehicle), we used cilia targeted Fe_2O_3-NPs without FD (control) and FD alone as another set of controls. Both Control and cilia targeted Fe_2O_3-NPs showed specific cilia targeted delivery, but only the presence of FD significantly increased the cilia length (**Figure. 3C**). Thus, FD was successfully released from cilia targeted Fe_2O_3-NPs and activated DR5 receptors. These results support the hypothesis that the activation of ciliary DR5 increases cilia length in embryonic fibroblasts, vascular endothelial cells and renal epithelial cells [6-8]. In addition to the fluorescence from cilia targeted Fe_2O_3-NPs, analyses of the ciliary marker acetylated-α-tubulin is to obtain more precise cilia length measurements (**Fig. 3C**).

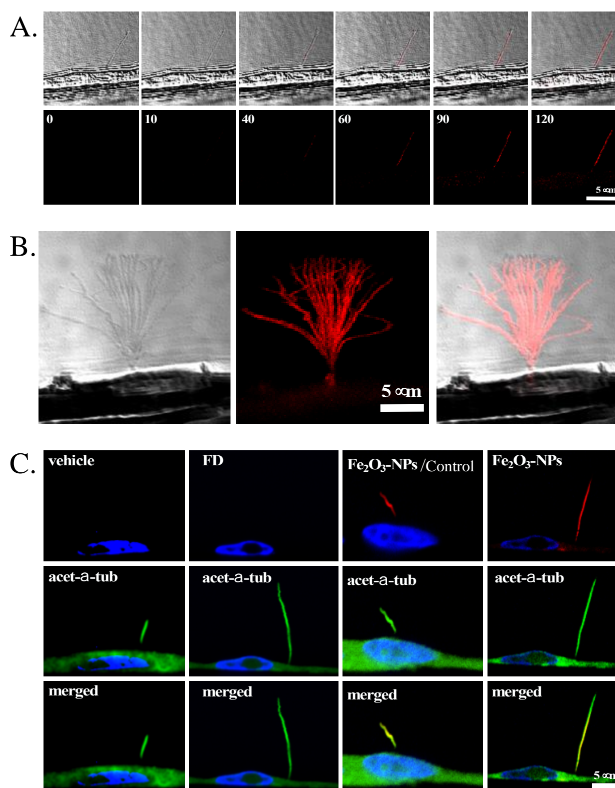

Figure 3. A) A side view cilium analysis was performed in a live cell to observe the targeting specificity of the cilia targeted Fe_2O_3-NPs at different time points. The top panel shows DIC images to confirm the presence of a cilium and fluorescence images to verify the cilia targeted Fe_2O_3-NP specificity. B) An external magnetic field acting on the cilia targeted Fe_2O_3-NPs/magnetic field induced passive cilia movements. C) Fluorescence images show that cilia length measurements compared with different treatments. The ciliary marker acetylated-α-tubulin (green) and a nuclear marker, DAPI, (blue) were used (adapted from [6]).

We next examined blood pressure to better understand ciliary function in the cardiovascular system. This was studied by injecting cilia targeted Fe_2O_3-NPs intravenously in the tail of an endothelial-specific *Pkd2* mouse model for 8 weeks (**Figure 4**).

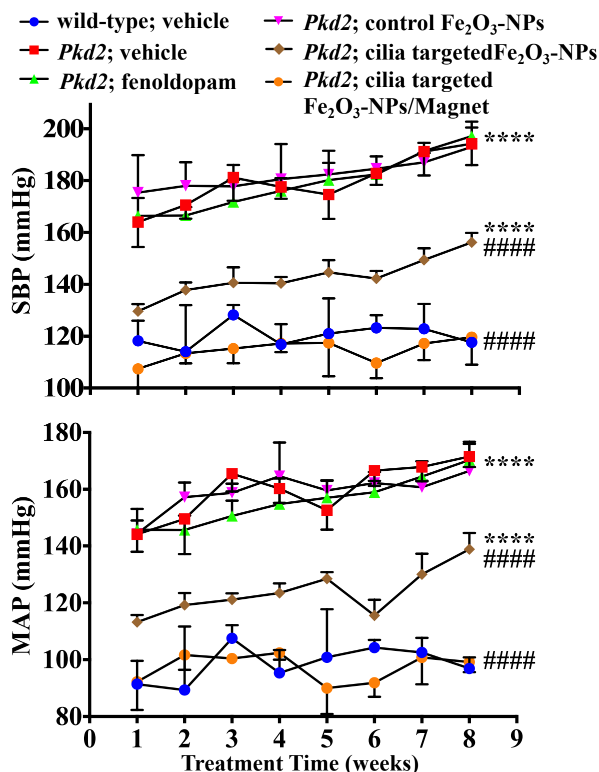

Figure 4. Blood pressure was measured at the end of each week for 8 consecutive weeks. Systolic blood pressure (SBP) and mean arterial pressure (MAP) are shown in the line graphs (adapted from [6]).

The cilia targeted Fe_2O_3-NPs significantly decreased the blood pressure of *Pkd2* mice. The cilia targeted Fe_2O_3-NPs under magnetic fields further decreased blood pressure, and it became comparable to normal wild-type mice (**Figure 4**). The administration of fenoldopam alone once every 3 days (a similar dosing regimen was used for cilia targeted Fe_2O_3-NPs) did not result in an overall decrease in systemic blood pressure. In separate studies, we confirmed that while FD alone decreased blood pressure, its affect only lasted for approximately one hour. Unlike the cilia targeted Fe_2O_3-NPs or cilia targeted Fe_2O_3-NPs/magnetic field, FD alone caused an immediate decrease in blood pressure, followed by reflex tachycardia. We speculated that this rebound in blood pressure and reflex tachycardia contributed to fenoldopam-induced mortality in hypertensive *Pkd2* mice. Based on the pharmacological profiles obtained from FD- and cilia targeted Fe_2O_3-NPs/magnetic field treated mice, both FD and the NPs remained in the circulatory system during the infusion.

4 CONCLUSIONS

In conclusion, we introduced a novel approach to target primary cilia for the very first time. FD was used as an experimental agent in the present study due to its therapeutic potential; unfortunately, it is limited by the requirement for a continuous infusion, non-selective activity and reflex tachycardia. With the unique cilia targeted system, we were able to encapsulate and deliver substances to cilia more precisely and effectively. Based on the findings from these studies, a ciliopathy treatment should not depend on generating new drugs if existing drugs are able to be specifically targeted to cilia for achieving the maximum therapeutic outcome with no side effects. Overall, cilia targeted delivery systems are an attractive means of achieving more targeted delivery of many other therapeutic pharmacological agents to treat various ciliopathies.

5 ACKNOWLEDGEMENTS

The research in our laboratory is funded by Congressionally Directed Medical Research Program PR130153 and the National Institutes of Health HL131577.

REFERENCES

[1] R. Pala, N. Alomari and S.M. Nauli. Int. J. Mol. Sci. 18, 2272, 2017.
[2] F.T. Chebib, C. R. Sussman, X. Wang, P.C. Harris and V.E. Torres. Nat. Rev. Nephrol. 11, 451−464, 2015.
[3] A.B. Chapman, K. Stepniakowski and F. Rahbari-Oskoui, Adv. Chronic. Kidney. Dis. 17, 153−163, 2010.
[4] R.J. Quinlan, J.L. Tobin and P.L. Beales, Curr. Top. Dev. Biol. 84, 249−310, 2008.
[5] R. Pala, M. Jamal, Q. Alshammari and S.M. Nauli. Cells 7, 233, 2018.
[6] R. Pala, A.M. Mohieldin, R.T. Sherpa, S.H. Kathem, K. Shamloo, Z. Luan, J. Zhou, J. Zheng, A. Ahsan, and Surya M. Nauli. ACS Nano, 13, 3555-3572, 2019.
[7] A. Marley and M. von Zastrow. PLoS One, 5, No. e10902, 2010.
[8] R. Pala, A.M. Mohieldin, K. Shamloo, R.T. Sherpa, S. H. Kathem, J. Zhou, Z. Luan, J. Zheng, A. Ahsan and S.M. Nauli. Nano Lett. 19, 904-914, 2019.